SEPARATION SCIENCE AND TECHNOLOGY
2020, VOL. 55, NO. 14, 2433–2448
https://doi.org/10.1080/01496395.2019.1634731

Taylor & Francis
Taylor & Francis Group

Adsorptive removal of alizarin dye from wastewater using maghemite nanoadsorbents

Ismail Badran and Rawan Khalaf

Department of Chemistry, An-Najah National University, Nablus, Palestine

ABSTRACT

This is an investigation of the adsorptive removal of anthraquinone dyes, resembled by Alizarin, by utilizing maghemite iron oxide (γ-Fe_2O_3) nanoparticles in aqueous media. The adsorption process was affected by several parameters such as solution pH, adsorbent amount, contact time, and temperature. After optimizing the parameters affecting the adsorption, the process was successful in removing Alizarin dye with an efficiency exceeding 95%. Best adsorption results were achieved at a pH of 11 and contact time of 60 min. The adsorption was shown to follow the Langmuir model suggesting a monolayer and homogeneous coverage. The maximum adsorption capacity (q_m) was found to be 23.2 mg/g at pH = 11. A thermodynamic study showed that the adsorption process is exothermic and spontaneous at room temperature. The Gibbs free energy of adsorption (-6.79 kJ/mol) obtained in this study suggests a physisorption process. This finding has facilitated the regeneration of the Fe_2O_3 nanocatalyst. Both NaOH and HNO_3 at dilute levels were tested for the regeneration of the nanocatalyst. Regeneration with HNO_3 was successful up to four successive removal cycles with an efficiency >80%. Photodegradation experiments utilizing a UV light were also successful in maximizing the adsorption removal efficiency. A sorption mechanism based on the results obtained in this work is also proposed.

ARTICLE HISTORY
Received 17 December 2018
Accepted 18 June 2019

KEYWORDS
Alizarin; Fe_2O_3; adsorption; regeneration; wastewater treatment

Introduction

Despite the fact that freshwater supply in our planet has remained fairly constant over time, it has become less accessible in recent years due to the growth in population, industrialization, and pollution. According to the United Nations, more than two billion humans lack access to safely managed water services in 2017.[1] In many areas, such as the Middle East and large parts of Africa, Droughts and contamination have affected both the quantity and quality of accessible water.[2,3] Organic dyes constitute a large portion of contaminates that contributes to freshwater quality.[4–7] They are sourced from textile, plastic, and cosmetic industries. Most dyes are not biodegradable, and many are suspected with carcinogenic and mutagenic effects.[8] The environmental impact of dyes pollution is enormous. It is estimated that the 800,000 tons of different dyes are produced globally every year[9]; of which, 17% to 20% is responsible for the total industrial water pollution according to the World Bank.[10]

Many technologies have been adapted to treat wastewater from organic pollutants, this includes electrochemical methods, coagulation–flocculation, precipitation, ion-exchange, membrane filtration, advanced oxidation, and adsorptive removal.[3,11–14] Due to its high efficiency, cleanness, and simplicity, adsorption succeeded as one of the most favored technologies in treat wastewater. Adsorption gained further importance with advancements in nanotechnology. In recent years, metal oxide nanoparticles (NPs) have demonstrated high efficiency in the adsorptive removal of both organic and inorganic wastes.[6,12,14–16] This is due to their large surface area, selectivity, and superior catalytic properties. Despite the extensive research on the adsorptive removal of organic waste, the large amount of "sludge" produced from the process is considered one of its major drawbacks. A new approach has been developed recently for the treatment of non-biodegradable organic matters present in industrial effluents "sludge".[5,17] This is achieved by using a new generation of nanoadsorbents, so-called, nanosorbcats, to first absorb the organic matter present in the wastewater onto the nanosorbcat surface, followed by upgrading this matter into new commodity chemicals or fuels. Upgrading can be achieved by either thermal oxidation, advanced oxidation, or catalytic cracking.

Anthraquinone dyes are classified as the second most important class after Azo dyes.[18] Examples of involve Purpurin, Morindon, Rubuadin, and Alizarin. In this

CONTACT Ismail Badran ibadran@ucalgary.ca Department of Chemistry, An-Najah National University, Nablus, PS, USA
Supplemental data for this article can be accessed on the publisher's website

work, we were motivated to choose Alizarin (ALZ), shown below, for two reasons; first, as a model for water-insoluble dyes, and, second, because of its unique chemical structure. ALZ consists of a fused three aromatic rings, with phenolic (-OH) and ketone (= O) functional groups. This type of structure can resemble the heavy aromatic waste found in tailing ponds, and as a by-product of heavy oil processing.[19,20]

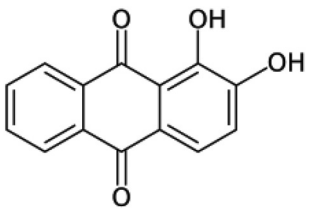

Chemical structure of Alizarin.

ALZ has many uses as a pigment, acid-base indicator, and in biological fields to identify calcium in tissue section.[21,22] The dye can be found in many forms, such as Alizarin red S (ARS), and Alizarin Yellow R (AYR), in addition to the parent ALZ shown above. Because of industrial importance, ALZ was a subject of several studies.[23–27] However, these studies were focused on ARS and AYR, rather than the parent ALZ itself. In addition, no attempt was made to develop a technique to treat this dye in acidic media, where its solubility is very low. In this work, we thoroughly investigated the adsorptive removal of ALZ from aqueous solutions using maghemite iron oxide (γ-Fe_2O_3) nanoparticles. The experimental parameters affecting the adsorption such as the pH, adsorbent amount, and contact time were optimized. A temperature study was also carried out in order to deduce the kinetic and thermodynamic parameter of adsorption. The Langmuir-Freundlich isotherm developed by Sips[28] was used to predict the adsorption behavior. In addition, the photodegradation of ALZ in the presence of γ-Fe_2O_3 nanoparticles was investigated using UV light, which decompose ALZ into simple products. A regeneration study for the NP catalyst was also performed by chemical etching, and the adsorption process was successful for four cycles using HNO_3 as etching agent.

The novelty of this work lies in two folds; first, it resembles the first study on the adsorptive removal of the parent ALZ dye. Secondly, it provides a comprehensive investigation for the adsorption mechanism, kinetics, and the regeneration of the γ-Fe_2O_3 NP catalyst, in addition to the enhanced removal utilizing UV light. The outcomes of the study are crucial for any future implementation of the process at the industrial scale.

Materials and methods

Chemicals

The γ-Fe_2O_3 nanoparticles (20–40 nm, surface area = 30–60 m^2/g) were purchased from Alfa Aesar, Massachusetts, USA. NPs from the same vendor were previously characterized by El-Qanni *et al.*[5] XRD analysis showed that the purchased NPs were free from any defects. Also, High-resolution TEM proved the spherical shape and the diameter of the NPs to be in the range of 5–15 nm, which is close to the size reported from the vendor. All other reagents including the ALZ dye, Borax, NaOH (99% pure), HCl (32% by mass), KH_2PO_4 (99% pure), KHP (98% pure), and acetic acid (98% pure) were purchased from Sigma-Aldrich Company Ltd, and were used as received without further purifications. These reagents were used to prepare the buffers required to regulate the solution pH.

Adsorption experiments

For the adsorption experiments described in this work, standard solutions of ALZ dye (240.21g/mol) were prepared in buffered solutions and using reagent grade deionized water. Different buffer solutions were used depending on the desired pH; KHP/NaOH buffer was used for pH = 3. Acetic acid/NaOH buffer for pH = 5, KH_2PO_4/HCl for pH = 7, Borax/HCl for pH = 9 and 9, and Borax/NaOH for pH>10. The final pH of the standard solution was adjusted using diluted HCl or NaOH. Batch adsorption experiments were carried out using 25 mL plastic vials. The vials, containing 10 mL of an aqueous solution and a specified amount of NPs were tightly sealed and shaken using Lab Tech® shaker (Daihan Labtech). The pH was adjusted and measured using JENWAY 3510 pH meter at the laboratory ambient temperature. In all experiments, the contaminated NPs were separated from treated media by using a small magnet bar, and the supernatant was decanted. No filtration was performed to avoid any side adsorption by filter papers. The concentration of ALZ in the supernatant was measured by UV-vis spectrophotometer (SHIMADZU UV-1800). Fourier transform infrared (FTIR) spectroscopy in the range (4000–400 cm^{-1}) was used for the characterization of ALZ and identify the changes on NPs before and after adsorption. FTIR Spectra were recorded using Thermo Scientific Nicolet IS5 spectrophotometer.

Adsorbent regeneration experiments

To test the reusability of the Fe_2O_3 NPs, 15 mg NPs were added to 10 ml dye solution (24.02 mg/L) and the mixture was shaken at 25°C for 4 hrs. After the magnetic separation, the supernatant was decanted and the contaminated NPs were collected by a magnet and washed with HNO_3. After that, the adsorbent was washed with distilled water and reused for adsorption again. The supernatant solutions were analyzed by UV–VIS spectrophotometer.

To study the effect of HNO_3 and NaOH on regeneration, several cycles of adsorption experiments were performed at different concentrations of the two reagents. A comparison was then made between the cycles to determine the etching reagents performance.

UV photodegradation experiments

The apparatus employed in the photocatalytic experiments is described in details elsewhere.[29] The setup consists of a high-pressure mercury UV light source (300 W, 230 V, ULTRA-VITALUX, OSRAM GmbH, Munich, Germany). The apparatus was placed in a sealed metal box to avoid the harmful UV radiation. In order to stabilize the temperature inside the chamber, a fan was fitted on the sidewall. The irradiation was concentrated on the reaction mixture using a lens.

Results and discussion

Optimizing adsorption parameters

Prior to each adsorption experiment on ALZ, a calibration curve was constructed using standard solutions of ALZ to quantify the concentration after adsorption. An example of the calibration curve is shown in the supplementary information section. For all calibration curves used in this work, a linear regression coefficient (R^2) close to unity was ensured for best results.

Adsorption experiments were performed with γ-Fe_2O_3 NPs as described in the experimental section. As shown in Fig. 1, adsorption was successful in treating the aqueous medium from the ALZ dye. Different environmental parameters were investigated to optimize the adsorption process. First, the effect of the amount of adsorbent was investigated by varying the amount of NPs in the range 1.0 to 45.0 mg in a 10 mL vials, and with a fixed dye concentration of 24.02 mg/L. Because of the fact that ALZ dye solubility in acidic medium is low, this part of the study was performed at a basic medium with pH = 11.0. The dye removal efficiency can be defined as:

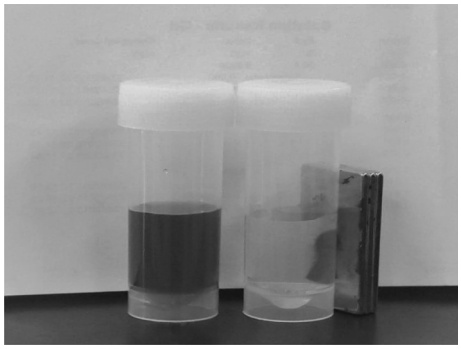

Figure 1. Photographs of ALZ sample before (right) and after shaking with γ-Fe_2O_3 NPs for 4 hrs. initial dye concentration = 24.02mg/L, solution's pH = 11, amount of adsorbent = 15 mg, shaking speed 130 rpm, 25^0C.

$$\%ofdyeremoval = \frac{C_o - C_e}{C_o} \times 100 \quad (1)$$

where C_o and C_e (mg/L) are the initial and equilibrium concentration of the dye in solution.

Figure 2 shows the increase in the removal efficiency as the amount of NPs becomes higher until the equilibrium limit. This is a common behavior of dyes adsorption on metal oxide NPs due to the increase in the number of active sorption sites as the amount of adsorbent becomes higher, till the sites are saturated.[30]

In order to better optimize the adsorption of ALZ, the effect of contact time on the removal efficiency was investigated by fixing all other parameters. It was found that the adsorption of ALZ increases quickly in the first 60 min, and then slows down until the adsorption process achieves equilibrium. Herein, it is worth noting that the fast removal rate during the first hour might be attributed to the rapid diffusion of ALZ from the solution to the external surface of the γ-Fe_2O_3 NPs. The short equilibrium time is in agreement with that reported by other studies. For instance, Nassar[15] investigated the removal of Pb(II) onto iron oxide NPs. It was reported that the rapid removal by the nanoparticles is due to their small size, which was favorable for the diffusion of adsorbate from bulk solution onto the active sites of the solid surface.[15,31] Meanwhile, as the sites being gradually occupied, the adsorbed ALZ tend to be transported slowly from the bulk solution to the actual occupied sorption sites. Such slow diffusion will decrease the adsorption rate of ALZ at later hours.

The next parameter we optimized is the pH of the solution, which is considered one of the very important parameters that affects the adsorption process. The adsorption of ALZ dye on Fe_2O_3 NPs was studied in acidic, neutral, and basic medium. As mentioned earlier, ALZ solubility in acidic medium is low, which introduced uncertainty in the quantification of ALZ at pH < 5. Therefore, the effect of pH on the adsorption of

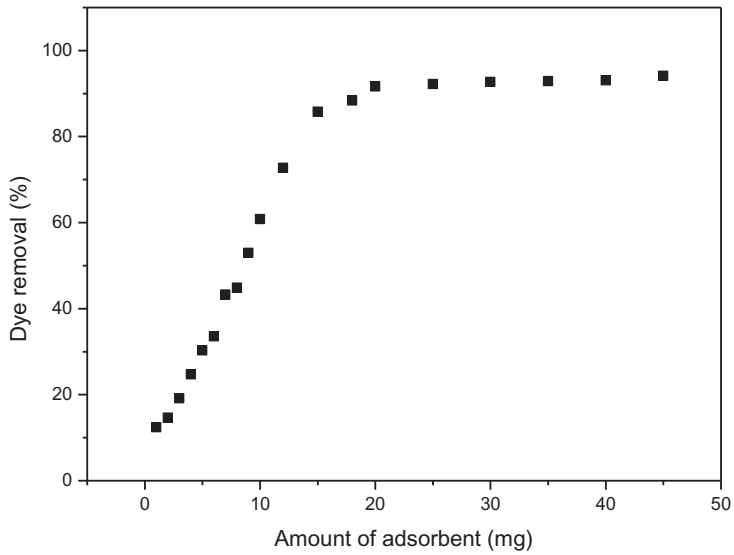

Figure 2. Effect of adsorbent amounts (mg) on removal efficiency of the ALZ, initial ALZ dye concentration 24.02mg/L, solution pH = 11, shaking time 4 hrs, 25^{0}C.

ALZ was studied in the pH range 8.0–12.0 as presented in Fig. 3. As seen, the removal of ALZ is highly pH dependent and increases with increasing pH. It was reported that the pH value of the point of zero charge (PZE) of γ-Fe_2O_3 NPs is 6.5.[32] At this value, the total positive charges on the surface of γ-Fe_2O_3 are equal to the total negative ones. Generally speaking, the adsorbent surface is positively charged when pH < pH_{pzc} because the acidic solution donates more protons than hydroxide groups. In contrast, when pH > pH_{pzc} the surface is negatively charged. Consequently, one can argue that the interaction of ALZ with the negatively charged Fe_2O_3 should increase with the increase of pH, leading to high adsorption. However, this was not the case in this work and an explanation of this phenomenon will be discussed later (Section 3.6).

Adsorption kinetics

Studying the adsorption kinetics helps in comprehending the adsorption mechanism. Also, such a study produces vital kinetic parameters, such as rate constants, that are required for any future industrial application of the process. The kinetics of ALZ adsorption was

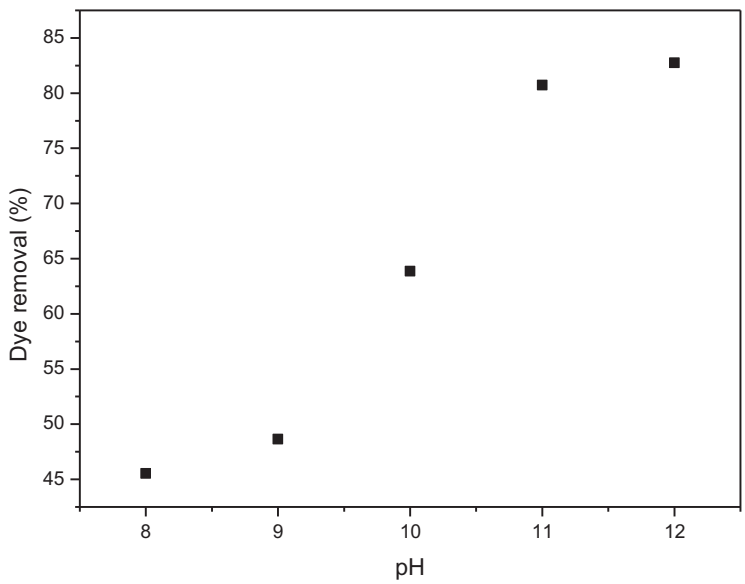

Figure 3. Effect of pH on the removal efficiency of ALZ dye at a fixed initial concentration of 24.02mg/L. shaking time = 4 hrs, shaking speed 130 rpm, 25°C.

studied by following the equilibrium adsorbate concentration (q_e), defined in eq. (2)[33,34,35] over a period of time. It is not uncommon in adsorption studies to use the Lagergren pseudo-first-order, and Ho pseudo-second-order rate equations given by Equations (3) and (4) follows:[33,35]

$$q_e = \frac{C_o - C_e}{W} V \tag{2}$$

$$\ln(q_e - q_t) = \ln q_e - k_1 t \tag{3}$$

$$\frac{1}{q_e - q_t} = k_2 t + \frac{1}{q_e} \tag{4}$$

where C_o, and C_e (mg/L) are the adsorbate initial concentration and at equilibrium, respectively. V(L) and W(g) are the solution volume and adsorbent dosage, respectively. q_e and qt (mg/g) are the adsorption capacities at equilibrium and time t, respectively, and k_1 and k_2 are the rate constant of the pseudo-first- and second-order of adsorption, respectively.

Figure 4 shows the time evolution of the equilibrium adsorbate concentration (q_e) up to 400 min. The experimental data in Fig. 4 were fitted to Equations (3) and (4) above using least square linear regression in Origin,[36] and the results are depicted in Fig. 5. By comparing the R-squared (R^2) regression values for the first-order (0.887) and the second-order (0.992) fittings, it is clear that the ALZ adsorption follows second-order kinetics, with an estimated pseudo-rate constant of 3.7×10^{-3}g/mg min. The pseudo-second-order kinetics of ALZ dye observed in this work is in agreement with previous studies on Alizarin red S (ARS) done by Fu *et al.*,[24] Gholivand *et al.*,[25] and Machado *et al.*[26] This agreement indicates that the rate determining step in the adsorption reaction

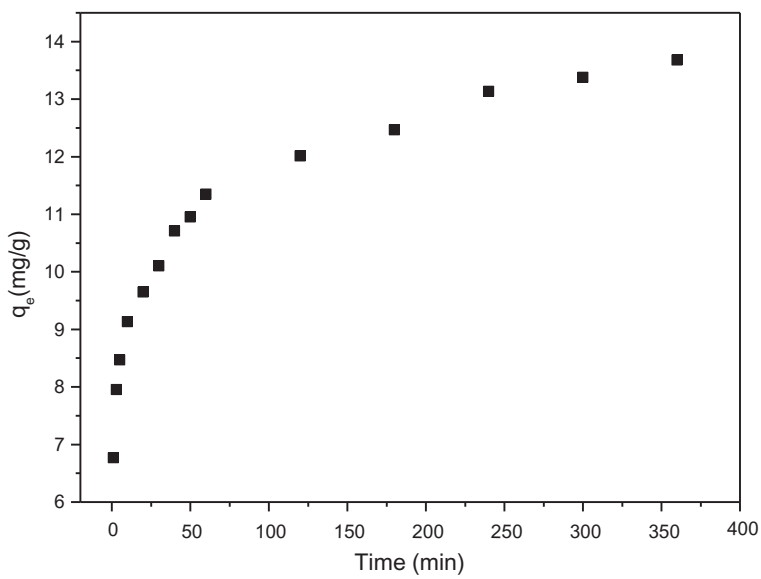

Figure 4. The change of the equilibrium adsorbate concentration (q_e) of ALZ with time, initial ALZ dye concentration 24.02mg/L, solution pH = 11, amount of adsorbent = 15 mg, shaking speed 130 rpm, 25^{0}C.

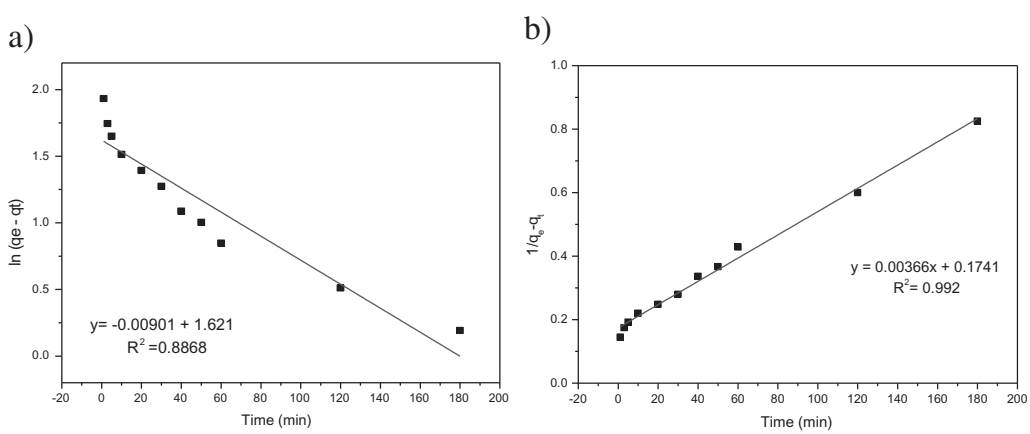

Figure 5. (a) Pseudo-first-order kinetics, and (b) pseudo-second-order kinetics of ALZ adsorption on Fe_2O_3 NPs.

involves a bimolecular interaction between the dye and the Fe_2O_3 NPs.

As seen from Fig. 2, the adsorption efficiency is >95% for an initial connotation of ALZ dye of 24.02 mg/L. In addition, the maximum adsorption capacity (q_{max}) obtained in this work at pH = 11 was determined to be 23.2 mg/g. These results are compared to previous studies in Table 1. As we mentioned in the introduction, there is plenty of studies that cover the adsorption of ARS and AYR dyes, while little work was done on the parent ALZ dye itself.

As seen from Table 1. The removal efficiency obtained in this work is comparable to those obtained in other adsorption, membrane filtration, or electrocoagulation studies. Also, the adsorption capacity value 23.2 mg/g obtained in this work is considered very good provided the low initial concentration of ALZ dye (24 mg/L).

The data tabulated in Table 1 suggests that the method used in this work is as efficient as other methods. However, non-adsorptive methods (membrane filtration, electrocoagulation, photodegradation, etc.), require costly parts and heavy setups. Therefore, adsorption is still considered advantageous, especially, when the highly effective, commercially available, and cheap γ-Fe_2O_3 NP is used.

Adsorption isotherms

The removal efficiency of any adsorbent depends on its capability of accumulating the adsorbate on its surface.[12,15] Adsorption isotherms, which are constant-temperature mathematical relationships between the amount of adsorbate per unit of adsorbent (q_e) and its equilibrium concentration (C_e), are of great significance in the adsorption process.[41] The importance of such isotherms is not limited to assess the adsorption efficiently, but also in designing efficient batch, continuous, or fixed-bed industrial adsorbers.[12,41] Therefore, we studied the adsorption isotherm of ALZ dye on the Fe_2O_3 NPs at different pH values and at different initial concentrations of ALZ ranging from 2.40 to 96.08 mg/L, as depicted in Fig. 6.

The two famous adsorption isotherms, Langmuir and Freundlich, were used to fit the experimental data obtained in this work. The Langmuir model assumes that all of the adsorption sites are equivalent and the monolayer adsorption occurs at the binding sites with homogenous energy levels and without any phase transition, *i.e.* no transmigration of adsorbed molecules on the adsorption surface. Also, Langmuir assumes that there are no interactions between adsorbed molecules.[42] The Langmuir equations can be expressed as[43,44]:

$$q_e = \frac{q_m K_L C_e}{1 + K_L C_e} \tag{5}$$

or

$$\frac{C_e}{q_e} = \frac{1}{K_L q_m} + \frac{1}{q_m} C_e \tag{6}$$

where C_e is the equilibrium concentration of the ALZ solution (mg/L), q_e is the adsorption capacity at equilibrium (mg/g), K_L is the constant related to free energy of adsorption (L/mg), and q_m (mg/g) is the maximum adsorption capacity, representing the maximum amount of ALZ adsorbed per unit weight of nanoadsorbents for complete monolayer coverage.

Figure 7(a) shows the results of fitting the experimental data in Fig. 6 according to the Langmuir model in Equation (6) using least square linear regression. By fitting C_e against C_e/q_e, a good linear relationship was obtained, and the values of K_L and q_m were determined from the intercept and slope of the plot. Here, the parameter q_m (mg/g) represents the maximum adsorption capacity of dye per unit mass of sorbent to form a complete monolayer on the surface bound at high C_e. Also, K_L (L/mg) represents the Langmuir energy

Table 1. Comparison between the results obtained in this work with previous studies.

Method	Dye	Initial Concentration mg/L	Adsorption efficiency (%)	Adsorption capacity q_{max} (mg/g)	Reference
Adsorption/Maghemite Fe_2O_3	ALZ	24	95%	23.2	Current Work
Adsorption/Magnetic activated carbon (MAC)/maghemite Fe_2O_3 nano-composite	ARS	70	99.4%	108.7	Fayazi *et al.*[23]
Adsorption/Activated clay modified by iron oxide (Fe-clay)	ARS	400	90%	32.7 mg/g	Fu *et al.*[24]
Adsorption/Polypyrrole-coated Fe_3O_4 nanoparticles	ARS	100	78.7%	116.3 mg/g	Gholivand *et al.*[25]
	AYR	120	97.8%	113.6 mg/g	
Adsorption/Single carbon nanotubes (SWCNT)	ARS	100–1000	95%	312.5	Machado *et al.*[26]
Adsorption/Multiwalled carbon nanotubes (MWCNT,)	ARS	100–1000	95%	135.2	Machado *et al.*[26]
Nano filtration/poly(piperazine amide) memebrane	AYR	100	97%	-	Lü *et. al.*,[37]
Electrocoagulation/aluminium electrodes	ARS	100	97%	785	Adeogun *et. al.*,[38]
Electrocoagulation/Fe/Al composite	ARS	300	90%	-	Ma *et. al.*,[39]
Electrocoagulation/aluminium electrodes	ARS	10–30	90%	-	Mukherjee *et. al.*,[40]

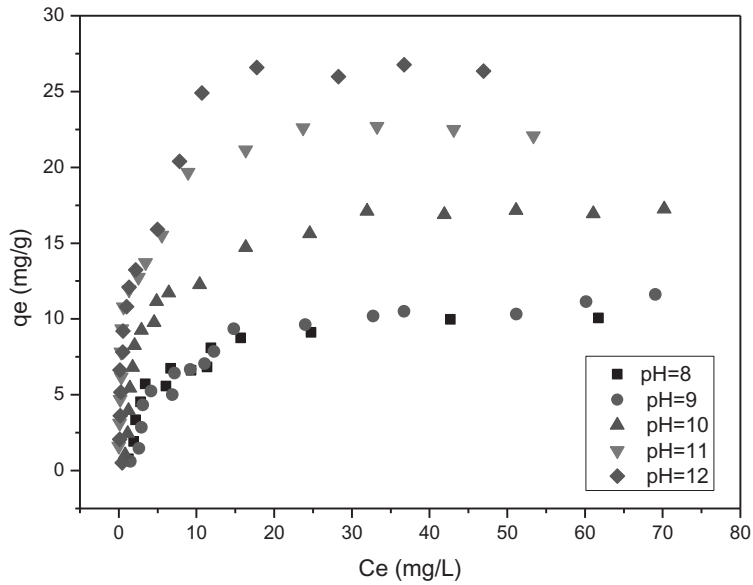

Figure 6. Adsorption isotherms of ALZ onto NPs at different pH values. Shaking time = 4 hrs, amount of adsorbent = 15 mg, shaking speed 130 rpm, 25°C.

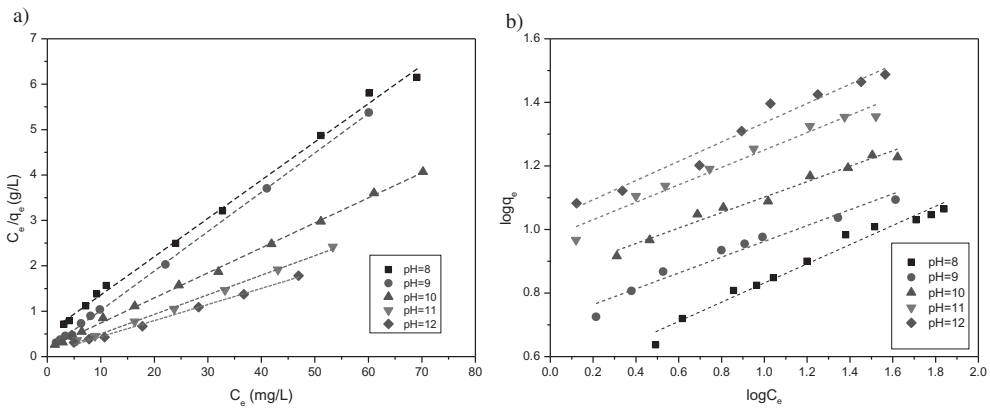

Figure 7. a) Langmuir isotherms, and b) Freundlich isotherms of ALZ onto NPs at different pH values. Shaking time = 4 hrs, amount of adsorbent = 15 mg, shaking speed 130 rpm, 25°C.

constant which is related to the heat of adsorption. The Langmuir parameters, K_L and q_m, in addition to the corresponding R^2values obtained from Fig. 7 shows are tabulated in Table 2. At pH = 12, q_m was found to be 28.6 mg/g.

In addition to the Langmuir isotherm, the experimental data obtained during this work were fitted to the Freundlich isotherm.[12,13,41] This is an empirical relationship describes the multilayer adsorption of heterogeneous systems and assumes that different sites have several adsorption energies involved. The corresponding equations are commonly represented by:

$$q_e = K_f C_e^n \tag{7}$$

or

$$\log q_e = \log K_f + n \log C_e \tag{8}$$

Thus, a plot of log C_e against log q_e should produce a straight line where the Freundlich constants, K_f and n, can be obtained from the intercept and slope. Here, K_F (1/g) is the Freundlich adsorption coefficient that characterizes the strength of adsorption. The higher the

Table 2. Fitting parameters for the Langmuir and Freundlich models at different pH values.

	Langmuir constants			Freundlich constants		
pH	K_L	q_m	R^2	K_F	n	R^2
8.0	0.161	11.904	0.995	3.380	0.301	0.972
9.0	0.547	11.905	0.995	5.164	0.248	0.956
10.0	0.286	18.181	0.997	7.211	0.243	0.978
11.0	0.614	23.255	0.998	9.462	0.274	0.961
12.0	0.406	28.571	0.991	10.764	0.303	0.963

value of F, the higher is the adsorbent loading that can be achieved.[41] The exponent, n, represents the adsorption intensity that varies with the heterogeneity of the adsorbate. In theory, n can take any value. In practice, however, Freundlich isotherms with $n < 1$ show relative high adsorbent loadings and considered favorable. Whereas isotherms with $n > 1$ are considered unfavorable.[41] Fig. 7(b) shows the fitting the data in Fig. 6 to the Freundlich isotherm modeled by Equation (8) using the least square linear regression. The parameters obtained from this fitting, K_f and n, are also tabulated in Table 2. As seen in the table, the adsorption of ALZ was fitted well with the Langmuir isotherm model with R^2 close to 0.99. This indicated that adsorption took place at specific homogeneous sites within the NPs adsorbent forming a monolayer coverage. The fact that ALZ dye adsorption on γ-Fe_2O_3 NP surface follows the Langmuir model is in complete agreement with previous studies performed on Alizarin dyes utilizingγ-Fe_2O_3 nanoparticles as adsorbents. Such as in the works of Fu *et al.*,[24] Fayazi *et al.*,[23] and others.[6,27] In addition, the Freundlich constant n was determined to be around 0.3. This value indicates a very favorable adsorption isotherm, as indicated earlier.[41,45]

To further understand the adsorption behavior, the experimental data obtained in this work were fitted to the SIPS isotherm.[28] This isotherm is a combination of the Langmuir and Freundlich isotherms and is valid for localized adsorption without adsorbate-adsorbate interactions.[46] When adsorbate concentrations C_e is low, it reduces to Freundlich isotherm; while at high concentrations, it predicts a monolayer adsorption capacity characteristic of the Langmuir isotherm. The general form of the SIPS isotherm is:[46]

$$q_e = q_m K_s C_e^{1/n} / \left(1 + K_s C_e^{1/n}\right) \tag{9}$$

where K_s (1/mg) and q_{max}(mg/g) are the SIPS equilibrium constant and maximum adsorption capacity values. The SIPS isotherm equation is characterized by the dimensionless heterogeneity factor, n, which can also be employed to describe the system's heterogeneity as n varies between 0 and 1.[47] When n is unity, it implies a homogeneous adsorption process approaching the Langmuir behavior. A nonlinear fitting of the experimental data obtained in this work to the SIPS model, Equation (9), is shown in Fig. 8. Also, Table 3 lists the different SIPS parameters obtained from the fitting. Clearly, the q_m values indicate that the adsorption capacity increases with increasing solution pH, in concert with our earlier findings. In addition, the values of the SIPS parameter, n, obtained in this work were close to unity, as seen in Table 3. This strongly suggests a homogeneous adsorption process, in agreement with our previous discussion that the adsorption follows Langmuir isotherm.

Adsorption thermodynamics

Temperature has been recognized as an important parameter governing the adsorption process.[13,41] Understanding the effect of temperature is not only needed to construct the adsorption mechanism but

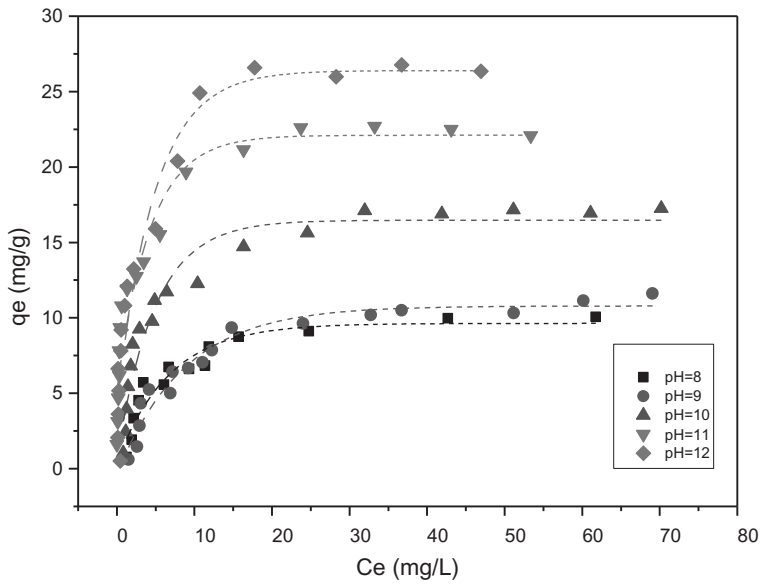

Figure 8. Non-linear fitting for SIPS isotherms of ALZ onto NP's at different pH values. Shaking time = 4 hrs, amount of adsorbent = 15 mg, shaking speed 130 rpm, 25^{0}C.

Table 3. Fitting parameters for the SIPS model at different pH values.

	SIPS constants				
pH	K_s	1/n	n	q_m	R^2
8.0	2.647	0.925	1.081	10.313	0.970
9.0	2.112	0.935	1.069	11.359	0.968
10.0	1.780	0.975	1.025	17.108	0.980
11.0	1.306	0.932	1.072	23.325	0.990
12.0	0.807	0.948	1.054	28.563	0.994

also to obtain some important thermodynamic parameters such as the standard Gibbs free energy, enthalpy and entropy changes accompanying adsorption.[48] Needless to say, changing the temperature may affect the equilibrium adsorption capacity of the adsorbent. For instance, the adsorption capacity will decrease upon increasing the temperature for an exothermic reaction, while it will increase for an endothermic one.[15]

In this study, the adsorption of ALZ dye on NPs was studied at the temperatures of 298, 313, and 328 K, the results are illustrated in Fig. 9.

As seen, the amount of ALZ adsorbed decreases as the temperature increases. This decrease in ALZ removal suggests that the adsorption of ALZ onto the NP's surface is an exothermic process. This behavior was an object of discussion in several studies. Alkan *et al.*,[49] reported that decreasing the adsorption with increasing temperature is mainly due to the weakening of adsorptive forces between the active sites of adsorbent and adsorbate species. So that, the adsorption of ALZ onto γ-Fe_2O_3 NPs decreases which in turn affect the removal efficiency of ALZ from wastewater sources. Similar observations were also discussed in the works of Juang *et al.*,[50]and Nassar.[6] Further insight towards the sorption mechanism will be discussed in Section 3.6

The experimental data obtained at a different temperature from Fig. 9 were analyzed to determine the thermodynamic parameters, such as the standard Gibbs free energy (ΔG°), standard enthalpy (ΔH°), and standard entropy (ΔS°) of adsorption. The importance of determining these parameters is not limited to describing the nature of adsorption, but also in providing the knowledge required to construct the adsorption mechanism.

The thermodynamic parameters, ΔG°, ΔH°, and ΔS° were calculated by the following equations:

$$\Delta G^{\circ} = \Delta H^{\circ} - \mathrm{T}\Delta S^{\circ} \tag{10}$$

$$\Delta G^{\circ} = -RTlnK \tag{11}$$

$$\ln K = -\frac{\Delta H^{\circ}}{RT} + \frac{\Delta S^{\circ}}{R} \tag{12}$$

where T is the temperature in Kelvin, R is the ideal gas constant (8.314 J/mol K), K is the equilibrium constant (dimensionless), which can also be expressed as $K_L \times C_s$, where K_L is the equilibrium Langmuir constant (L/mmol) and C_s is the solvent molar concentration (mM).

The values of ΔS° and ΔH° can be determined by plotting *lnK* versus *1/T* as presented in Fig. 10. From the slope and intercept in the figure, ΔH° and ΔS° were calculated using Equation (12). The thermodynamic parameters ΔG°, ΔH°, and ΔS° were estimated at -6.79 kJ/mol, -27.82 kJ/mol, and -70.98 J/mol.K, respectively.

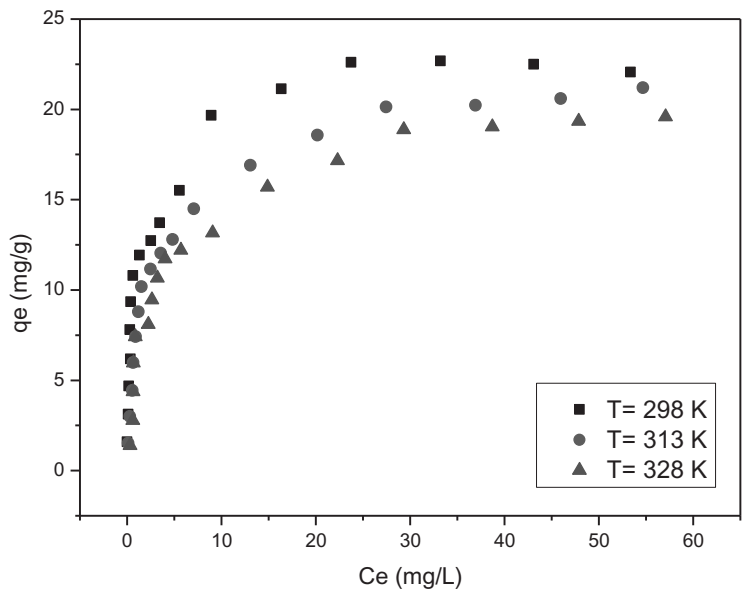

Figure 9. Adsorption isotherms of ALZ onto NPs at different temperatures. Shaking time = 4 hrs, amount of adsorbent = 15 mg, shaking speed 130 rpm.

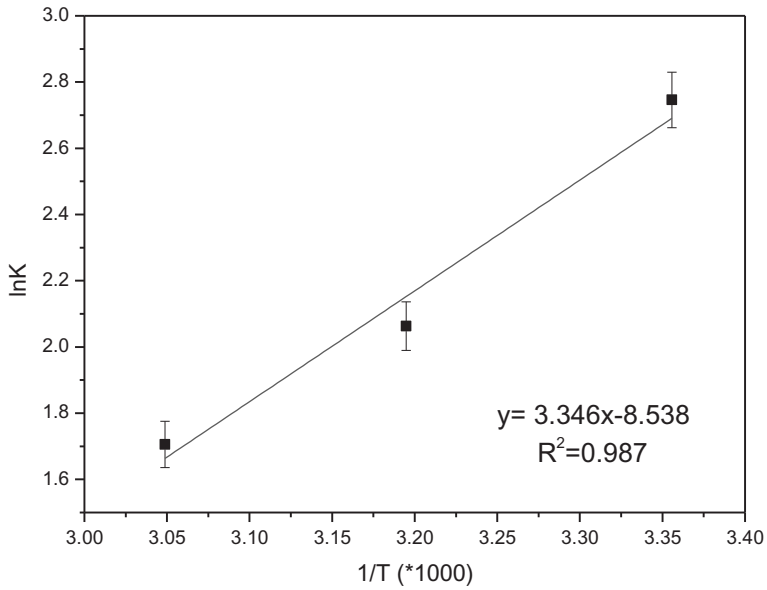

Figure 10. Determination of thermodynamic parameters for the adsorption of ALZ onto Fe_2O_3 NPs.

The negative ΔG° and ΔH° values obtained in this work indicate that the adsorption of ALZ dye onto the Fe_2O_3 NPs is exothermic and spontaneous at room temperature. This explains why the adsorption was favored at low temperatures as we discussed earlier. The negative value of ΔS° value, -70.98 J/mol K indicates that the randomness decreases at the NPs interface as adsorption proceeds as expected, which adds a driving force for the negative Gibbs-free energy and the spontaneity of the adsorption. However, the small magnitude of ΔG° indicates a weak adsorptive force between the active sites of adsorbent and the ALZ dye. According to Yu *et al.*,[51] ΔG° values between −20 and 0 kJ/mol correspond to physisorption while that with values between −80 and −400 kJ/mol corresponds to the chemisorption process. The relatively small ΔG° value obtained in this study strongly suggests a physisorption process for ALZ dye. Furthermore, several studies related the standard enthalpy of adsorption (ΔH°) to the nature of the adsorption process. For instance, Bride *et al.*[52] suggested that a value of ΔH° lower than 40 kJ/mol corresponds to a physisorption. The ΔH° value obtained in this study (-27.82 kJ/mol) supports our conclusion that the adsorption process of ALZ dye on Fe_2O_3 NPs is a physisorption process.

FTIR investigation of NPs adsorbents

In order to have a close look at the adsorption mechanism, an FTIR characterization was performed on the pure ALZ dye, along with the Fe_2O_3 NPs before and after adsorption, as detailed in the experimental section. Figure S2-a in the supplementary information section presents the FTIR spectra for pure γ- Fe_2O_3 NPs. As seen, the spectrum shows no major peaks in the region 1000–4000 cm^{-1}, which confirms that the NPs surface is free from any organic contamination prior to adsorption. The FTIR spectrum for pure ALZ dye is shown in Figure S2-b. The IR peak around 1630 $cm^{-1}$is assigned to aromatic C = C stretching vibration.[53] The peak around 1660 cm^{-1} corresponds to carbonyl C = O bond stretching vibration.[53] The broad peak at 3370 cm^{-1} is assigned to phenolic O-H group stretching. The strong peak at 1290 cm^{-1} can be attributed to C = C stretching within the aromatic structure of ALZ, and the peak at 1450 cm^{-1} can also be attributed to phenolic O-H group bending.[53] After adsorption, the NPs were filtered, washed, and dried. An FTIR spectrum for contaminated NPs was collected and is shown in Figure S2-c. It is clear that there are no major differences between the two spectra of the Fe_2O_3 NPs before and after adsorption. This confirms our previous finding that the adsorption of ALZ on the NPs surface is a physical phenomenon that is ruled by weak attractions, rather than strong chemical interactions between the NP adsorbent and the ALZ adsorbate molecules. Furthermore, the retain of the O-H peak at 3370 cm^{-1}after adsorption indicates that the OH functional group is the one that responsible for the electrostatic attraction between negatively charged adsorbate molecules and positively charged adsorbent active sites.

Mechanism of sorption

In the previous sections, the results of different environmental parameters on the adsorption of ALZ dye

were presented. It was determined that that adsorption is pH dependent and the % removal increases with pH. This observation is in contradiction with previous studies on some organic dyes. For instance, in his study on the adsorptive removal of acid red using γ-Fe_2O_3 NPs, Nassar[6] found that the adsorption efficiency drops with increasing pH. Also, Fayazi *et al.*[23] found that the removal efficiency of ALZ red S (ARS) using activated carbon/γ-Fe_2O_3 nano-composite was also decreasing with increasing pH. Gholivand *et. al.* reported the same observation on their study on ARS and AYR as well.[25] To explain this contradiction, we propose the sorption mechanism in Scheme 1. In contrast to the anionic dyes, Acid red, ARS and AYR, the parent ALZ molecular structure contains two hydroxyl (-OH) groups that makes it a weak acid. The first deportation step takes place in acidic medium (pKa_1 = 5.3)[54] followed by the loss of another proton at higher pH (pKa_1 = 11.5).[54] As inspired by Pirillo *et. al.*[54], both alizarin anions, I and II, are able to interact with the Fe_2O_3 NP surface via hydrogen bonds (Scheme 1), One can argue that the parent ALZ molecule can also interact via H-bonding through its two – OH groups. However, and as we mentioned earlier, the solubility of ALZ in acidic medium is very low, mostly due to its large aromatic system. ALZ is more soluble in the basic medium due to its transformation to the anionic forms, I and II, as illustrated in Scheme 1. This explains why ALZ adsorption on the γ-Fe_2O_3 surface is low in acidic media.

It is noteworthy to mention that the enhanced adsorption of ALZ on Fe_2O_3 surface at high pH is in concert with methyl violet (MV) adsorption on the same adsorbent. In their 2016 study, Tong *et al.* explained this behavior by the fact that MV is a cationic dye, and deprotonation at higher pH leads to stronger attraction with the Fe_2O_3 surface.[55]

It is well known that the γ-Fe_2O_3 surface is negatively charged at pH > 6.5, which is the point of zero change.[32] Since the two anionic forms, I and II, bear also negative charges, one can argue that the repulsion forces between the surface and the ALZ anions should hinder the adsorption process at higher pH values. This dilemma can be clarified by the fact that ALZ

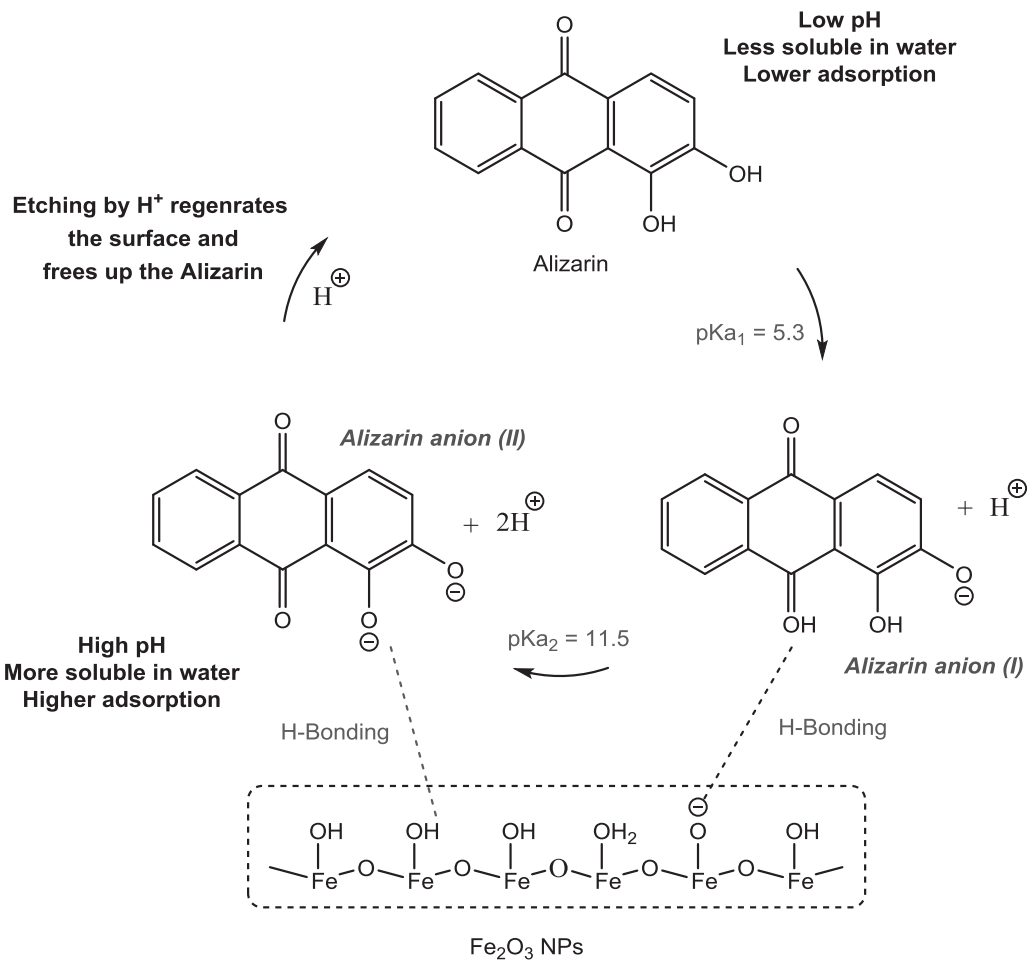

Scheme 1. Proposed mechanism for the sorption/desorption of Alizarin dye.

adsorption is of physisorption nature. Earlier in Section 3.4, the adsorption was found to be exothermic and ruled by physical (physisorption) forces rather than chemical ones. In such a case, weak physical attractions overcome electrostatic bonding.

Finally, the adsorption was shown to follow the Langmuir model (Section 3.3). This infers a homogeneous, and monolayer coverage on the active sites. The fact that the molecules of the two negatively charged anions, I and II, are unable to attract each other's through with electrostatic forces, explains this Langmuir behavior. Once the first adsorption layer is formed, the molecules would not be able to aggregate to form a second or third layer.[41]

Finally, Scheme 1 suggests that the presence of excess H^+ ions will recycle the two anionic forms, I and II, back to the neutral ALZ molecule. This should desorb the ALZ from the iron oxide surface and. At the end of this paper, we show that this is indeed possible and a strong acid, such as HNO3, can be used to regenerate the catalyst surface.

Regeneration of adsorbent

Based on the above results, we foresee adsorption as a promising process for the removal of Anthraquinone dyes, resembled by ALZ, from wastewater. The adsorption process was proven to be simple, clean, efficient, and utilizing low-cost γ-Fe_2O_3 nanoparticles. In order to make this process more environment-friendly, the regeneration of the adsorbent is a necessity that determines the cost-effectiveness and the reuse of the adsorbent.

In the previous section, we showed that the adsorption of ALZ dye to γ-Fe_2O_3 NPs surface is physical. That is the adsorptive forces between adsorbent and adsorbate are weak and can be broken easily. This facilitated the regeneration process and make is it feasible. Also, it was shown that the adsorption is highly pH dependent, and the removal efficiency improves as the solution becomes more basic. Consequently, the desorption of ALZ can be carried out by decreasing the pH of the solution. This suggests that washing the contaminated NPs with an acidic solution is helpful in their regeneration. In this study, we separated and washed the Fe_2O_3 NPs with dilute solutions of NaOH, and HNO_3. The regenerated NPs were used again for another adsorption cycle. Figure 11 shows the removal efficiency as a function of NaOH or HNO_3 concentration. As seen, the efficiency of NPs after regeneration using HNO_3 is higher than that of NaOH. Also, the results revealed that the efficiency of the regenerated NPs has increased as the HNO_3 concentration becomes lower. This result can be rationalized on entropy bases. As the concentration of HNO_3 becomes more diluted, the difference in entropy (ΔS) between the adsorbed dye species and the bulk solution increases. This creates the driving force for more ALZ species to escape the NPs surface into the bulk solution.

Using a diluted solution of 10 mM HNO_3, the maximum numbers of adsorption-desorption cycles were investigated. As shown in Fig. 12, the regeneration was successful up to four successive removal cycles

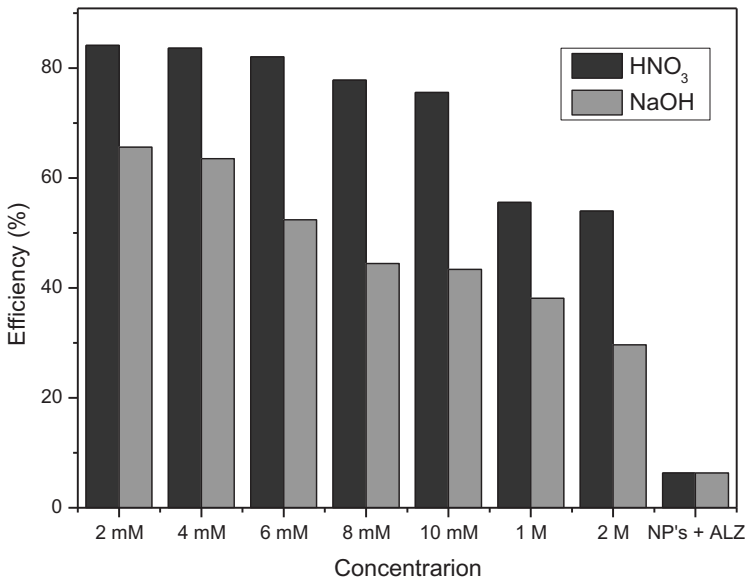

Figure 11. Removal efficiency of NP after regeneration using different concentrations of NaOH and HNO_3 solutions at a fixed initial concentration of ALZ:12 mg/L, pH = 11, shaking rate: 130 rpm, shaking-contact time: 4 h, 25°C.

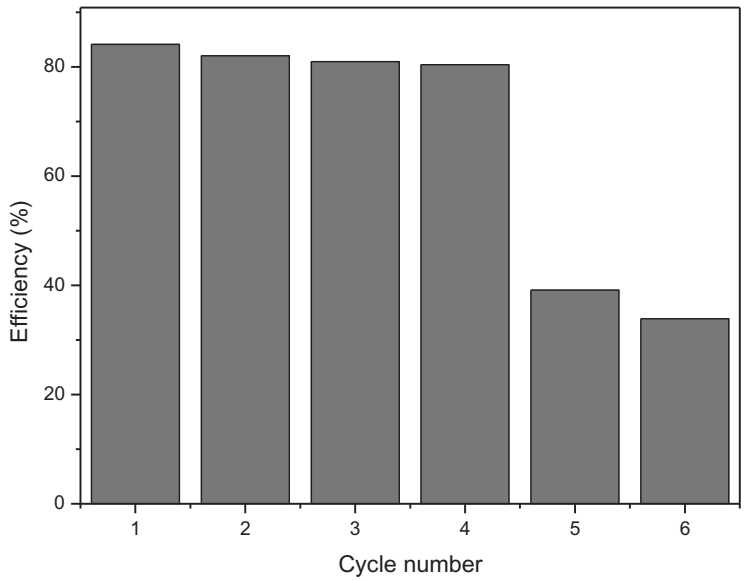

Figure 12. Reusability of Fe_2O_3 NPs for adsorption/desorption of ALZ during six adsorption-desorption cycles using 10 mM HNO_3. Initial concentration of ALZ: 12 mg/L, amount of adsorbent:15 mg, pH = 11, shaking rate: 130 rpm, shaking-contact time: 4 h, 25°C.

with an efficiency higher than 80%. After that, the removal efficiency drops to 40%.

Effect of UV-light

The concept of nanosorbcat, a nano-adsorbent that works as a catalyst, introduced earlier in the introduction, involves a selective adsorption of the pollutant on a nano surface, followed by upgrading into valuable commodity or fuel.[5,56] We tested the catalytic activity of the γ-Fe_2O_3 NPs as potential nanosorbcat by studying the adsorption of ALZ dye under direct and indirect sunlight, and under UV light, as detailed in the experimental section. Figure 13 illustrates the results of this study. It is clear from the figure that removal efficiency has increased from *ca.* 60% to >95% when UV light was used. In addition, the efficiency was as low as 40% in the dark. This proves that UV light has enhanced the removal efficiency of ALZ dye by the Fe_2O_3 NPs. Although the energy band gap in Fe_2O_3 NPs is estimated at 2.2 eV, which corresponds to absorption in the visible region of the spectrum (560 nm). The

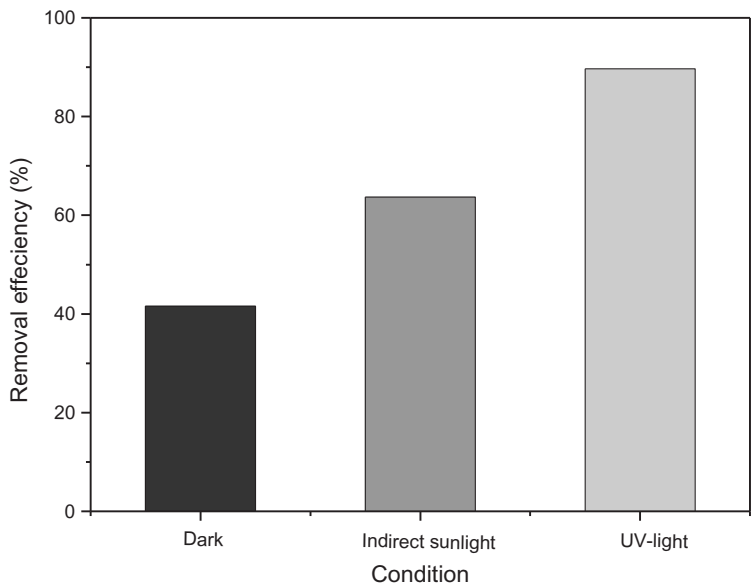

Figure 13. Effect of UV-light on adsorptive removal of ALZ onto γ-Fe_2O_3 NPs. Initial concentration of ALZ: 24 mg/L, amount of adsorbent:15 mg, pH = 11, stirring time: 2 h, 25°C.

enhanced activity of the nanoparticles when the UV lamp was used is attributed to both the high intensity and frequency of photons generated by the UV light.

The results obtained in this work agree well with a recent study by Saeed *et al.*,[57] where photodegrading of ARS dye was also enhanced in basic medium. The authors denoted this to the possible increase to the OH• radicals formed at high pH. It is noteworthy to mention that OH• radicals play the essentials role in the photodegradation reactions of organic compounds.[57–62]

Conclusions

This study showed that γ-Fe_2O_3 NPs could be used as both a nanoadsorbent and a catalyst (nanosorbcat) for the adsorptive removal of ALZ dye from an aqueous solution within short contact time with nearly complete removal. The effect of various parameters were investigated and the results showed that the adsorption process was dependent on the amount of γ-Fe_2O_3 NPs, contact time, solution pH, and temperature. The adsorption efficiency was shown to increase with higher amount of adsorbent. A proposed sorption mechanism explains this observation by the fact that ALZ is slightly soluble in acidic medium, and the formation of anionic structures at high pH. Maximum removal was obtained at pH = 11 with a maximum adsorption capacity (q_m) of 23.2 mg/g. A UV-light irradiation increased the adsorptive removal without affecting the magnetic properties and adsorption capacity of γ-Fe_2O_3. This result confirmed the catalytic properties of the γ-Fe_2O_3 NPs. The adsorption equilibrium was also investigated and described by Freundlich, Langmuir, and SIPS models. The adsorption data were shown to fit the Langmuir isotherm indicating a homogenous coverage. A comparison of kinetic models on the overall adsorption rate showed that ALZ dye/γ-Fe_2O_3 adsorbent system was best described by the pseudo-second-order rate model. The thermodynamic study of ALZ adsorption onto the γ-Fe_2O_3 indicated that the process is exothermic, and spontaneous at room temperature. The physisorption nature of the adsorption process indicated that weak interactions exist between the adsorbent and adsorbate moieties. Thus, a desorption and regeneration process is feasible. Hence, regeneration studies were carried out using HNO_3 and confirmed that the γ-Fe_2O_3 can be reused up to four cycles. In conclusion, γ-Fe_2O_3 NP are proven to be effective and inexpensive adsorbents and their regeneration is simple. The results obtained in this work confirm that the adsorption process using γ-Fe_2O_3 nanosorbcats is efficient, simple, and cost-effective and can be easily scalable industrial level.

Acknowledgements

The authors are grateful to the Faculty of Science at An-Najah National University for funding and supporting this research. R. Khalaf is thankful to the generous financial support provided by the Middle East Desalination Research Center (MEDRC) fellowship. The authors are thankful to Dr. Hikmat Hilal for providing access to the UV lamp used in this project.

Funding

This work was supported by the MEDRC.

ORCID

Ismail Badran http://orcid.org/0000-0003-1423-7124
Rawan Khalaf http://orcid.org/0000-0002-5470-0876

References

[1] Progress on Drinking Water, Sanitation and Hygiene: 2017 Update and SDG Baselines. Geneva: World Health Organization (WHO) and the United Nations Children's Fund (UNICEF), 2017.
[2] Postel, S.;. *The Last Oasis: Facing Water Scarcity*; Routledge, New York, NY, 10017, USA, 2014.
[3] Feng, Y.; Yang, L.; Liu, J.; Logan, B. E. Electrochemical Technologies for Wastewater Treatment and Resource Reclamation. *Environ. Sci.* 2016, 2(5), 800–831.
[4] Robinson, T.; McMullan, G.; Marchant, R.; Nigam, P. Remediation of Dyes in Textile Effluent: A Critical Review on Current Treatment Technologies with a Proposed Alternative. *Bioresour. Technol.* 2001, 77(3), 247–255.
[5] El-Qanni, A.; Nassar, N. N.; Vitale, G.; Hassan, A. Maghemite Nanosorbcats for Methylene Blue Adsorption and Subsequent Catalytic Thermo-Oxidative Decomposition: Computational Modeling and Thermodynamics Studies. *J. Colloid Interface Sci.* 2016, 461, 396–408. DOI: 10.1016/j.jcis.2015.09.041.
[6] Nassar, N. N.;. Kinetics, Mechanistic, Equilibrium, and Thermodynamic Studies on the Adsorption of Acid Red Dye from Wastewater by γ-Fe2O3 Nanoadsorbents. *Sep. Sci. Technol.* 2010, 45(8), 1092–1103. DOI: 10.1080/01496391003696921.
[7] The Current Status of Industrial Sector in Palestine. In The Palestinian Federation of Industries: 2009.
[8] Bahram, M.; Asadi, S.; Karimnezhad, G. Synthesized Poly Styrene-Alt-Maleic Acid Hydrogel for Removal of Azo Dyes, Methylene Blue and Methyl Orange, from Aqueous Media. *J. Iran. Chem. Soc.* 2015, 12(4), 639–645. DOI: 10.1007/s13738-014-0522-7.
[9] Hassaan, M. A.; El Nemr, A. Health and Environmental Impacts of Dyes: Mini Review. *Am. J. Environ. Sci. Eng.* 2017, 1(3), 64–67.
[10] Kant, R.;. Textile Dyeing Industry an Environmental Hazard. *Nat. Sci.* 2012, 4(1), 22–26. DOI: 10.4236/ns.2012.41004.
[11] Ngah, W. W.; Hanafiah, M. Removal of Heavy Metal Ions from Wastewater by Chemically Modified Plant

Wastes as Adsorbents: A Review. *Bioresour. Technol.* 2008, 99(10), 3935–3948. DOI: 10.1016/j.biortech.2007.06.011.

[12] Nassar, N. N.;. *The Application of Nanoparticles for Wastewater Remediation*; Applications of Nanomaterials for Water Quality. Future Science Book Series: Future Science Ltd; 2013. p. 52-65

[13] Yang, R. T.;. *Adsorbents: Fundamentals and Applications*; Wiley-Interscience: Hoboken,N.J, 2003.

[14] Qu, X.; Alvarez, P. J.; Li, Q. Applications of Nanotechnology in Water and Wastewater Treatment. *Water Res.* 2013, 47(12), 3931–3946. DOI: 10.1016/j.watres.2012.09.058.

[15] Nassar, N. N.;. Rapid Removal and Recovery of Pb (II) from Wastewater by Magnetic Nanoadsorbents. *J. Hazard. Mater.* 2010, 184(1–3), 538–546. DOI: 10.1016/j.jhazmat.2010.08.069.

[16] Carlos, L.; Einschlag, F. S. G.; González, M. C.; Mártire, D. O. Applications of Magnetite Nanoparticles for Heavy Metal Removal from Wastewater. In *Waste Water-Treatment Technologies and Recent Analytical Developments*; InTech, 2013.

[17] Marei, N. N.; Nassar, N. N.; Hmoudah, M.; El-Qanni, A.; Vitale, G.; Hassan, A. Nanosize Effects of NiO Nanosorbcats on Adsorption and Catalytic Thermo-Oxidative Decomposition of Vacuum Residue Asphaltenes. *Can. J. Chem. Eng.* 2017, In Press. DOI:10.1002/cjce.22884.

[18] Bien, H. S.; Stawitz, J.; Wunderlich, K. Anthraquinone Dyes and Intermediates. Ullmann's Encyclopedia of Industrial Chemistry, 2000, Wiley-VCH Verlag GmbH & Co. KGaA, Weinheim, Germany. DOI:10.1002/14356007.a02_355

[19] Adams, J. J.;. Asphaltene Adsorption, a Literature Review. *Energy Fuels*. 2014, 28(5), 2831–2856. DOI: 10.1021/ef500282p.

[20] Badran, I.; Nassar, N. N.; Marei, N. N.; Hassan, A. Theoretical and Thermogravimetric Study on the Thermo-Oxidative Decomposition of Quinolin-65 as an Asphaltene Model Molecule. *RSC Adv.* 2016, 6(59), 54418–54430. DOI: 10.1039/C6RA07761G.

[21] Ercoli, N.; Lewis, M. The Age Factor in the Response of Bone Tissue to Alizarin Dyes and the Mechanism of Dye Fixation. *Anat. Rec.* 1943, 87(1), 67–76. DOI: 10.1002/(ISSN)1097-0185.

[22] Pirillo, S.; Pedroni, V.; Rueda, E.; Luján Ferreira, M. Elimination of Dyes from Aqueous Solutions Using Iron Oxides and Chitosan as Adsorbents: A Comparative Study. *Quím. Nova*. 2009, 32(5), 1239–1244. DOI: 10.1590/S0100-40422009000500030.

[23] Fayazi, M.; Ghanei-Motlagh, M.; Taher, M. A. The Adsorption of Basic Dye (Alizarin Red S) from Aqueous Solution onto Activated carbon/γ-Fe2O3 Nano-Composite: Kinetic and Equilibrium Studies. *Mater. Sci. Semicond. Process.* 2015, 40, 35–43. DOI: 10.1016/j.mssp.2015.06.044.

[24] Fu, F.; Gao, Z.; Gao, L.; Li, D. Effective Adsorption of Anionic Dye, Alizarin Red S, from Aqueous Solutions on Activated Clay Modified by Iron Oxide. *Ind. Eng. Chem. Res.* 2011, 50(16), 9712–9717. DOI: 10.1021/ie200524b.

[25] Gholivand, M. B.; Yamini, Y.; Dayeni, M.; Seidi, S.; Tahmasebi, E. Adsorptive Removal of Alizarin red-S and Alizarin Yellow GG from Aqueous Solutions Using Polypyrrole-Coated Magnetic Nanoparticles. *J. Environ. Chem. Eng.* 2015, 3(1), 529–540. DOI: 10.1016/j.jece.2015.01.011.

[26] Machado, F. M.; Carmalin, S. A.; Lima, E. C.; Dias, S. L.; Prola, L. D.; Saucier, C.; Jauris, I. M.; Zanella, I.; Fagan, S. B. Adsorption of Alizarin Red S Dye by Carbon Nanotubes: An Experimental and Theoretical Investigation. *J. Phys. Chem. C.* 2016, 120 (32), 18296–18306. DOI: 10.1021/acs.jpcc.6b03884.

[27] Absalan, G.; Bananejad, A.; Ghaemi, M. Removal of Alizarin Red and Purpurin from Aqueous Solutions Using Fe3O4 Magnetic Nanoparticles. *Anal. Bioanal. Chem. Res.* 2017, 4(1), 65–77. DOI: 10.22036/abcr.2017.41099

[28] Sips, R.;. On the Structure of a Catalyst Surface. *J. Chem. Phys.* 1948, 16(5), 490–495. DOI: 10.1063/1.1746922.

[29] Zyoud, A. H.; Zaatar, N.; Saadeddin, I.; Ali, C.; Park, D.; Campet, G.; Hilal, H. S. CdS-sensitized TiO2 in Phenazopyridine Photo-Degradation: Catalyst Efficiency, Stability and Feasibility Assessment. *J. Hazard. Mater.* 2010, 173(1–3), 318–325. DOI: 10.1016/j.jhazmat.2009.08.093.

[30] Bharathi, K.; Ramesh, S. Removal of Dyes Using Agricultural Waste as Low-Cost Adsorbents: A Review. *Appl. Water Sci.* 2013, 3(4), 773–790. DOI: 10.1007/s13201-013-0117-y.

[31] Uheida, A.; Salazar-Alvarez, G.; Björkman, E.; Yu, Z.; Muhammed, M. Fe3O4 and γ-Fe2O3 Nanoparticles for the Adsorption of Co2+ from Aqueous Solution. *J. Colloid Interface Sci.* 2006, 298(2), 501–507. DOI: 10.1016/j.jcis.2005.12.057.

[32] Jarlbring, M.; Gunneriusson, L.; Hussmann, B.; Forsling, W. Surface Complex Characteristics of Synthetic Maghemite and Hematite in Aqueous Suspensions. *J. Colloid Interface Sci.* 2005, 285(1), 212–217. DOI: 10.1016/j.jcis.2004.11.005.

[33] Qiu, H.; Lv, L.; Pan, B.-C.; Zhang, Q.-J.; Zhang, W.-M.; Zhang, Q.-X. Critical Review in Adsorption Kinetic Models. *J. Zhejiang Univ. Sci. A.* 2009, 10(5), 716–724. DOI: 10.1631/jzus.A0820524.

[34] Ho, Y. S.; McKay, G. A Comparison of Chemisorption Kinetic Models Applied to Pollutant Removal on Various Sorbents. *Process Saf. Environ. Prot.* 1998, 76 (4), 332–340. DOI: 10.1205/095758298529696.

[35] Ho, Y. S.; McKay, G. Sorption of Dye from Aqueous Solution by Peat. *Chem. Eng. J.* 1998, 70(2), 115–124. DOI: 10.1016/S0923-0467(98)00076-1.

[36] Origin, Version 8.5. OriginLab Corporation, Northampton, MA, USA.

[37] Lü, Z.; Hu, F.; Li, H.; Zhang, X.; Yu, S.; Liu, M.; Gao, C. Composite Nanofiltration Membrane with Asymmetric Selective Separation Layer for Enhanced Separation Efficiency to Anionic Dye Aqueous Solution.

J. Hazard. Mater. 2019, 368, 436–443. DOI: 10.1016/j.jhazmat.2019.01.086.

[38] Adeogun, A. I.; Balakrishnan, R. B. Electrocoagulation Removal of Anthraquinone Dye Alizarin Red S from Aqueous Solution Using Aluminum Electrodes: Kinetics, Isothermal and Thermodynamics Studies. *J. Electrochem. Sci. Eng.* 2016, 6(2), 199–213.

[39] Ma, S. S.; Gang Zhang, Y. Electrolytic Removal of Alizarin Red S by Fe/Al Composite Hydrogel Electrode for Electrocoagulation toward a New Wastewater Treatment. *Environ. Sci. Pollut. Res.* 2016, 23(22), 22771–22782. DOI: 10.1007/s11356-016-7483-6.

[40] Mukherjee, T.; Das, P.; Ghosh, S. K.; Rahaman, M. Removal of Alizarin Red S from Wastewater: Optimizing the Process Parameters for Electrocoagulation Using Taguchi Method. Waste Water Recycling and Management, 2019, 239–249, Springer, Singapore: Singapore. DOI: 10.1007/978-981-13-2619-6_19

[41] Worch, E.;. *Adsorption Technology in Water Treatment: Fundamentals, Processes*, and modeling. 2012. Berlin, Germany: De Gruyter.

[42] Ngah, W. W.; Hanafiah, M. Biosorption of Copper Ions from Dilute Aqueous Solutions on Base Treatedrubber (Hevea Brasiliensis) Leaves Powder: Kinetics, Isotherm, and Biosorption Mechanisms. *J Environ Sci.* 2008, 20(10), 1168–1176. DOI: 10.1016/S1001-0742(08)62205-6.

[43] Limousin, G.; Gaudet, J.-P.; Charlet, L.; Szenknect, S.; Barthes, V.; Krimissa, M. Sorption Isotherms: A Review on Physical Bases, Modeling and Measurement. *Appl. Geochem.* 2007, 22(2), 249–275. DOI: 10.1016/j.apgeochem.2006.09.010.

[44] Worch, E.;. *Adsorption Technology in Water Treatment: Fundamentals*, processes, and modeling. 2012. Berlin, Germany: De Gruyter.

[45] Allen, S.; Mckay, G.; Porter, J. F. Adsorption Isotherm Models for Basic Dye Adsorption by Peat in Single and Binary Component Systems. *J. Colloid Interface Sci.* 2004, 280(2), 322–333. DOI: 10.1016/j.jcis.2004.08.078.

[46] Foo, K. Y.; Hameed, B. H. Insights into the Modeling of Adsorption Isotherm Systems. *Chem. Eng. J.* 2010, 156(1), 2–10. DOI: 10.1016/j.cej.2009.09.013.

[47] Kumara, N.; Hamdan, N.; Petra, M. I.; Tennakoon, K. U.; Ekanayake, P. Equilibrium Isotherm Studies of Adsorption of Pigments Extracted from Kuduk-Kuduk (Melastoma Malabathricum L.) Pulp onto TiO2 Nanoparticles. *J. Chem.* 2014. DOI: 10.1155/2014/468975.

[48] Eren, E.;. Removal of Lead Ions by Unye (Turkey) Bentonite in Iron and Magnesium Oxide-Coated Forms. *J. Hazard. Mater.* 2009, 165(1–3), 63–70. DOI: 10.1016/j.jhazmat.2008.09.066.

[49] Alkan, M.; Demirbaş, Ö.; Celikcapa, S.; Doğan, M. Sorption of Acid Red 57 from Aqueous Solution onto Sepiolite. *J. Hazard. Mater.* 2004, 116(1–2), 135–145. DOI: 10.1016/j.jhazmat.2004.08.003.

[50] Juang, R.; Wu, F.; Tseng, R. The Ability of Activated Clay for the Adsorption of Dyes from Aqueous Solutions. *Environ. Technol.* 1997, 18(5), 525–531. DOI: 10.1080/09593331808616568.

[51] Yu, Y.; Zhuang, -Y.-Y.; Wang, Z.-H. Adsorption of Water-Soluble Dye onto Functionalized Resin. *J. Colloid Interface Sci.* 2001, 242(2), 288–293. DOI: 10.1006/jcis.2001.7780.

[52] McBride, M.B. Environmental chemistry of soils. 1994 . Oxford University Press, Inc., New York DOI:10.3168/jds.S0022-0302(94)77044-2

[53] Silverstein, R. M.; Webster, F. X.; Kiemle, D. J.; Bryce, D. L. *Spectrometric Identification of Organic Compounds*; John Wiley & Sons, 2014.

[54] Pirillo, S.; Ferreira, M. L.; Rueda, E. H. The Effect of pH in the Adsorption of Alizarin and Eriochrome Blue Black R onto Iron Oxides. *J. Hazard. Mater.* 2009, 168(1), 168–178. DOI: 10.1016/j.jhazmat.2009.02.007.

[55] Tong, Z.; Zheng, P.; Bai, B.; Wang, H.; Suo, Y. Adsorption Performance of Methyl Violet via α-Fe 2O3@ Porous Hollow Carbonaceous Microspheres and Its Effective Regeneration through a Fenton-Like Reaction. *Catalysts*. 2016, 6(4), 58. DOI: 10.3390/catal6040058.

[56] Marei, N. N.; Nassar, N. N.; Hmoudah, M.; El-Qanni, A.; Vitale, G.; Hassan, A. Nanosize Effects of NiO Nanosorbcats on Adsorption and Catalytic Thermo-Oxidative Decomposition of Vacuum Residue Asphaltenes. *Can. J. Chem. Eng.* 2017, 95(10), 1864–1874. DOI: 10.1002/cjce.v95.10.

[57] Saeed, K.; Zada, N.; Khan, I. Photocatalytic Degradation of Alizarin Red Dye in Aqueous Medium Using Carbon nanotubes/Cu–Ti Oxide Composites. In *Separation Science and Technology*, 2018; pp 1–9. doi:10.1080/01496395.2018.1552296.

[58] Navgire, M. E.; Lande, M. K. Effect of Nanocrystalline Composite Fullerene-Doped MoO3-TiO2 Material on Photoassisted Degradation of Alizarin Red S Dye. *Inorg. Nano-Metal Chem.* 2017, 47(3), 320–327. DOI: 10.1080/15533174.2016.1186055.

[59] Lachheb, H.; Puzenat, E.; Houas, A.; Ksibi, M.; Elaloui, E.; Guillard, C.; Herrmann, J.-M. Photocatalytic Degradation of Various Types of Dyes (Alizarin S, Crocein Orange G, Methyl Red, Congo Red, Methylene Blue) in Water by UV-irradiated Titania. *Appl. Catal. B Environ.* 2002, 39(1), 75–90. DOI: 10.1016/S0926-3373(02)00078-4.

[60] Badran, I.; Hassan, A.; Manasrah, A. D.; Nassar, N. N. Experimental and Theoretical Studies on the Thermal Decomposition of Metformin. *J. Therm. Anal. Calorim.* 2019. DOI: 10.1007/s10973-019-08213-9.

[61] Badran, I.; Manasrah, A. D.; Nassar, N. N. A Combined Experimental and Density Functional Theory Study of Metformin Oxy-Cracking for Pharmaceutical Wastewater Treatment. *RSC Adv.* 2019, 9(24), 13403–13413. DOI: 10.1039/C9RA01641D.

[62] Aoudjit, F.; Cherifi, O.; Halliche, D. Simultaneously Efficient Adsorption and Photocatalytic Degradation of Sodium Dodecyl Sulfate Surfactant by One-Pot Synthesized TiO2/layered Double Hydroxide Materials. *Sep. Sci. Technol.* 2019, 54(7), 1095–1105. DOI: 10.1080/01496395.2018.1527352.